

Synthesis and characterization of visible light active S-doped TiO₂ nanophotocatalyst

S. Janitabar Darzi ^{*1}; A. R. Mahjoub ²; A. Bayat ²

¹Nuclear Science and Technology Research Institute, 11365/8486 Tehran, Iran

²Department of Chemistry, Tarbiat Modares University, 14115-175 Tehran, Iran

Received 19 April 2015; revised 28 August 2015; accepted 20 September 2015; available online 14 November 2015

ABSTRACT: S-doped and baremesoporous TiO₂ were prepared using titaniumtetraisopropoxide and thiocarbamide as raw materials. Prepared materials were characterized by means of fourier transform infrared spectroscopy FT-IR, thermogravimetry-differential scanning calorimetry (TG-DSC), X-ray diffraction (XRD), UV-Vis absorption spectroscopy, Brunauer–Emmett–Teller (BET) specific surface area and Barrett–Joyner–Halenda (BJH) pore size distribution analyses, scanning electron microscopy (SEM) and Energy-dispersive X-ray spectroscopy (EDX). The band gap of S-doped was estimated from UV-Vis spectroscopy data to be 2.8 eV. The specific surface area of S-doped TiO₂ nanoparticles obtained via the BET method, calculated to be 181.3 m²/g and its pore size distribution curve revealed that the average diameter of the pores is 12.3 nm using BJH method. Photocatalytic efficiency of synthesized S-doped mesoporous TiO₂ was tested for degradation of Congoredazo dye under ultraviolet and visible lights. The results revealed that the S-doped mesoporous TiO₂ is the most effective under visible light in comparison with bare one.

Keywords: Band gap; Congored; Mesoporous; Photocatalyst; S-doped; TiO₂.

INTRODUCTION

Titanium dioxide (TiO₂) is highlighted as an important semiconductor photocatalyst because of its superior characters such as exceptional optoelectronic property, strong oxidizing power, chemical stability, low cost, and so on [1, 2]. However, the photocatalytic activity of TiO₂ is not high enough to be suitable for commercial application. One major restriction in utilizing of this semiconductor is related to its wide band gap energy, causing TiO₂ not be able to generate photoexcited electrons and holes to promote red-ox reactions unless it is irradiated by ultraviolet light [3]. Another drawback of this semiconductor is a fast recombination of its photogenerated charges (electrons and holes) which decrease photocatalytic efficiency of TiO₂.

In recent years, many efforts have been directed toward shifting the optical sensitivity of the TiO₂ from UV to the visible-light spectrum for the efficient use of

solar radiation or artificial visible light [4]. It is generally agreed that the presence of metal or nonmetal dopants into TiO₂ lattice increases the photocatalytic activity of the material under visible light irradiation [5- 7]. On the other side, producing porous TiO₂ samples with large surface area can improve its photocatalytic properties by means of reducing the recombination rate of photo induced electron-hole pairs. This is due to their faster arrival to the reaction site of the surface and efficient charge separation which increases the lifetime of the charge carriers and enhances the photocatalytic efficiency [8].

The doping of non-metal elements such as N, F, S and P in TiO₂ lattice can lower its band gap and shift its optical response to the visible light region [9, 10]. Ohno et al. reported that S cation-doped TiO₂ powder absorbed visible light more strongly than N, C and the S anion-doped TiO₂ powders also showed photocatalytic activity under visible light [11]. However, sulfur doping TiO₂ has small specific surface area and low adsorption capability, which results in poor photocatalytic efficiency when the contaminant

✉ *Corresponding Author: Simin Janitabar-Darzi

Email: sjanitabar@aeoi.org

Tel.: (+98) 2182063410

Fax: (+98) 2188221116

concentration is low [12]. The pending problem is how to improve the visible light photocatalytic efficiency of doping TiO₂ towards low concentration solution, because some contaminants are harmful to people, animals and plants even at low concentration.

In this work S-doped mesoporous TiO₂ and a bare mesoporous TiO₂ were prepared using a simple sol-gel method. The photocatalytic efficiency of synthesized nonmaterial was tested for degradation of Congoredazo dye under ultraviolet and visible lights.

EXPERIMENTAL

Materials and Apparatus

All the raw materials used in this work were bought from Merck company. Spectroscopic analyses of mesoporous bare TiO₂ and S-doped TiO₂ were performed using Bruker Equinox 55 FT-IR spectrometer. Powder phase identification was performed by X-ray diffraction (XRD) obtained on Philips X-pert diffractometer using Cu K α line ($\lambda = 1.54056 \text{ \AA}$) radiation, working with voltage and current of 40 kV and 40 mA. UV-vis spectrophotometer (Shimadzu UV 2100) was applied for the study of photodegradation reactions. Brunauer-Emmett-Teller (BET) specific surface area and Barret-Joyner-Halenda (BJH) pore size distribution of the S-doped TiO₂ nanoparticles was determined through nitrogen adsorption (Quantachrome NOVA 2200 e). The morphology of the prepared photocatalysts was investigated by scanning electron microscopy (SEM, Philips XL30). Oxford INCA energy-dispersive X-ray (EDX) was used to analyze the elemental constituents of S-doped TiO₂ nanoparticles.

Preparation of S-doped TiO₂ and bare mesoporous TiO₂ nanoparticles

Preparation of the S-doped TiO₂ nanoparticles was started by dissolving 3 g of triblock copolymer EO₂₀-PO₇₀-EO₂₀ (P123) and a proper amount of thiourea in 170 mL of absolute ethanol under vigorous stirring. Another solution by mixing 0.02 mol of titanium tetraisopropoxide (Ti(OCH(CH₃)₂)₄, TTIP), 0.01 mol of acetylacetone, and 30 mL of ethanol was prepared then mixed with the first solution. The produced mixture was stirred for 2 h. The produced dispersion was treated by HCl and pH adjusted to 1.5. The mixture was hydrolyzed in this acidic medium under 3 h gentle stirring. After that, the solution was aged for 48 h to obtain a gel and then dried at 100 °C for 24 h. Finally, it calcined at 450 °C for 1 h.

Bare mesoporous TiO₂ was prepared by triblock copolymer EO₂₀-PO₇₀-EO₂₀ (P123) surfactant and titanium tetraisopropoxide as starting materials. 3 g of Pluronic P-123 was dissolved in 200 mL ethanol. The resulting solution was stirred for 1 h. Then 0.02 mol of titanium tetraisopropoxide under vigorous stirring was added to above clear solution. The mixture was maintained in a beaker for 5 h under gentle stirring. After that, the mixture was dried at 100 °C for 32 h to obtain a gel, and then calcined at 500 °C for 1 h.

Photocatalytic Activity Determination

Photocatalytic experiments were performed in an open Pyrex vessel filled with 100 mL of aqueous suspension of Congored (5 ppm) containing 0.05 g/L of photocatalysts and the UV radiation source, a lamp (30 W, UV-C, $\lambda = 253.7 \text{ nm}$, manufactured by Philips, Holland), was irradiated perpendicularly to the surface of photocatalyst solution. Two 18 W Osram lamps were used as the light source for visible light photocatalytic reactions and the distance between the irradiation source and vessel containing the reaction mixture was fixed at 2 cm. Air was blown into the reaction by an air pump during the course of the reaction. The experiments were performed at room temperature. Initially, the suspension was magnetically stirred in the dark for 30 min to ensure the establishment of an adsorption/desorption equilibrium among the photocatalyst particles, dye molecules, and atmospheric oxygen. During the course of light irradiation, a suspension of about 5 mL was taken out after regular time intervals. The suspension was centrifuged and then passed through milipore filters to remove suspended photocatalyst particles. Finally, the filtrates were studied by UV-Vis spectroscopy.

RESULTS AND DISCUSSION

Characterization of the photocatalysts

Fig. 1 a and b exhibits FT-IR spectrum of the S-doped TiO₂ photocatalyst, before and after calcination.

FT-IR spectrum of the S-doped TiO₂ before calcination (spectrum a) shows a broad peak at 3000–3600 cm⁻¹, which is assigned to the fundamental stretching vibration of hydroxyl groups (free or bonded) [13]. This is further confirmed by the weak band at about 1615 cm⁻¹ [14], which is as a result of bending vibration of coordinated H₂O as well as Ti-OH. The bending vibrational mode of water may appear as shoulders on the spectrum, as in 2800 cm⁻¹ [15]. It was reported that the vibration of the Ti-O bonds in the

TiO₂ lattice may be located at 500 and 430 cm⁻¹[13]. Other peaks are attributed to the P-123 surfactant. After calcinations (spectrum b), the absorption feature due to P-123 is almost removed, as evidenced by the significantly reduced characteristic bands at 2850, 2940 and 1080 cm⁻¹[16]. In the curve b, appearing shoulder at 1030 cm⁻¹ should be related to Ti–O–S, suggesting a conjugation effect between the S and Ti–O bonds. This finding is in accordance with Liu et al. report [17].

Differential thermal and thermogravimetric curves of the S-doped TiO₂ powder before the calculation are shown in Fig. 2. According to Thermogravimetry (TG) analysis, the weight loss consists of some distinct steps.

The first stage of weight loss corresponds to removal of physically absorbed water up to 100°C. The second step is regarding to evolution of CO₂ and carbonylsulfide at 140°C which reach the maximum rate

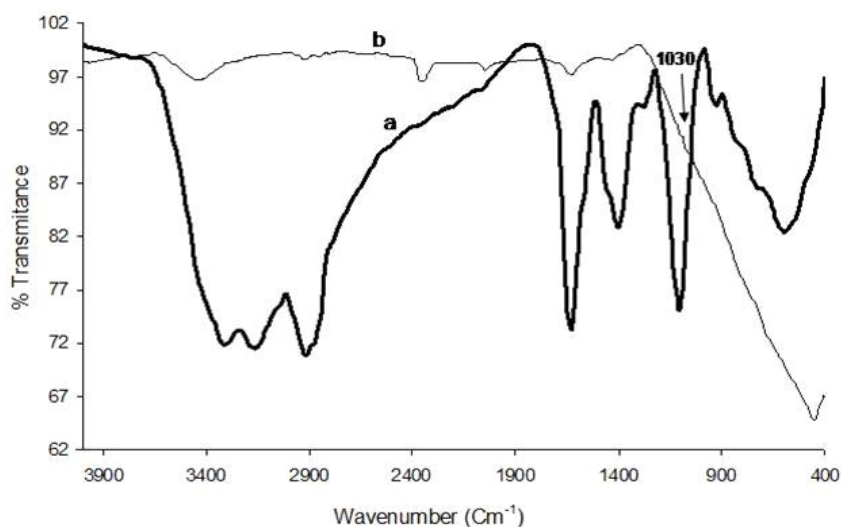


Fig. 1: FT-IR spectrum of the S-doped TiO₂ photocatalyst, before (a) and (b) after calcinations.

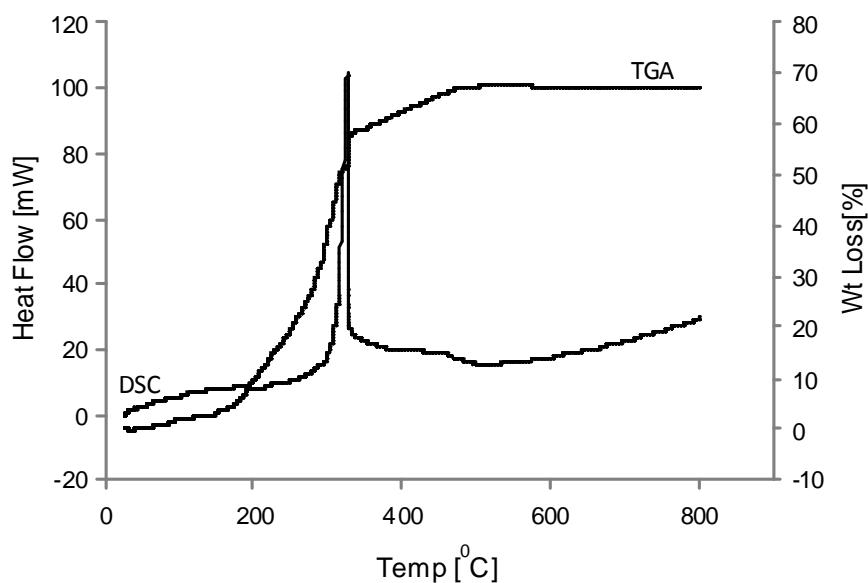


Fig. 2: Thermogravimetry-differential scanning calorimetry (TG-DSC) curves of the S-doped TiO₂ before calcination.

at 170°C and 180°C, respectively [18]. Also, Release of ammonia has been reported to occur from 170°C to 185°C. The significant exothermic peak in DSC curve at around 320°C corresponds to oxidation of NH₃ into N₂O and H₂O [18]. Finally, a weak thermal effect at 400–500 °C is accompanied by a diffuse exothermal peak at around 450 °C in the DSC curve which confirms the crystallization of the amorphous phase to anatase. The gel–crystalline conversion temperature has been reported to be 350–500 °C for TiO₂ prepared by the sol–gel method [19]. However, direct observation of the exothermic effect in the DSC curve has been difficult, probably because the crystallization temperature is usually close to the decomposition temperatures of residual surfactant, which are demonstrated as endothermic effects [8].

The crystalline structure of S-doped and bare TiO₂ nanoparticles was investigated by X-ray diffraction (XRD) measurements. The XRD patterns obtained from these samples are shown in Fig. 3. The X-ray diffraction results of samples indicated that both of S-doped and bare TiO₂ nanoparticles exhibited anatase

phase of TiO₂ and doping with sulfur does not change the crystal structure of TiO₂. The average crystallite size of bare TiO₂ and S-doped TiO₂ samples were calculated by Scherrer's equation to be 28.32 and 23.81 nm, respectively.

SEM images of S-doped TiO₂ and bare TiO₂ nanoparticles were presented in Fig. 4a and b. According to SEM images, the samples are granular and the obtained S-doped TiO₂ nanoparticles are approximately 10 nm in diameter. Combined with the result of XRD, it is obvious that the agglomeration was significant for bare TiO₂ compared to S-doped TiO₂. So, S-doping can reduce the agglomerate size of TiO₂. EDX analysis of S-doped sample (Fig. 5) exhibits that the prepared matter is composed of a small amount of sulfur element.

The optical band gap (E_g) in a semiconductor was determined by plotting (αhν)^{1/m} versus photon energy (hν) where α represents optical absorption coefficient and m represents the nature of transition. Now, m may have different values, such as 1/2, 2, 3/2 or 3 for allowed direct and indirect; and forbidden direct and indirect

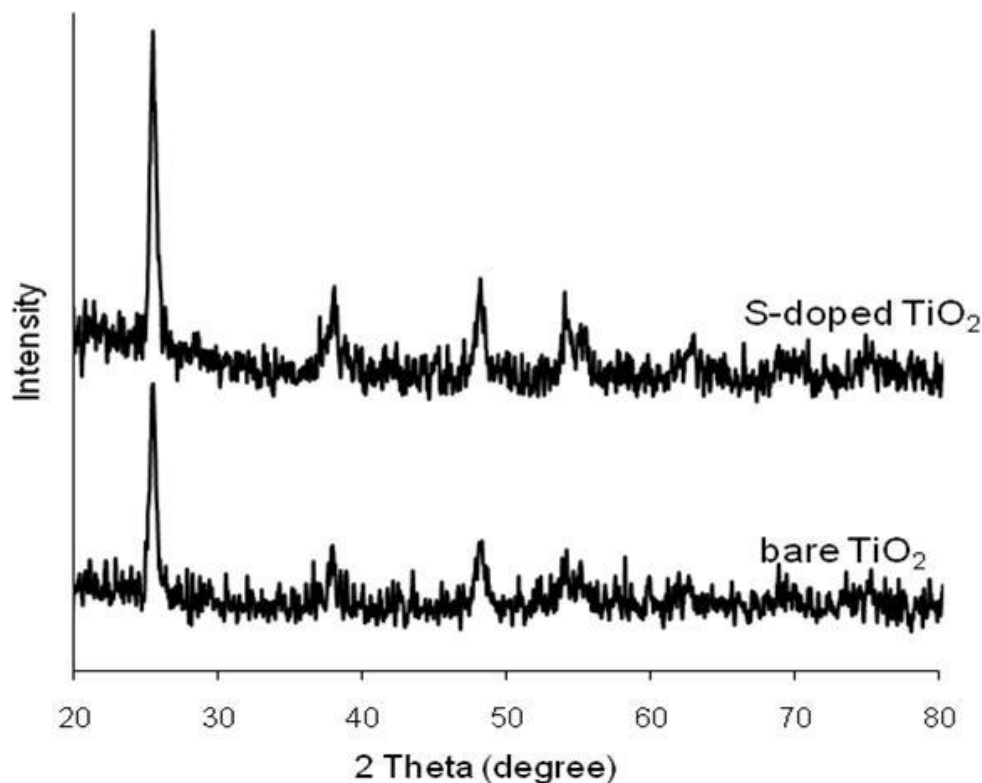


Fig. 3: XRD patterns of the S-doped (a) and bare (b) TiO₂ nanoparticles.

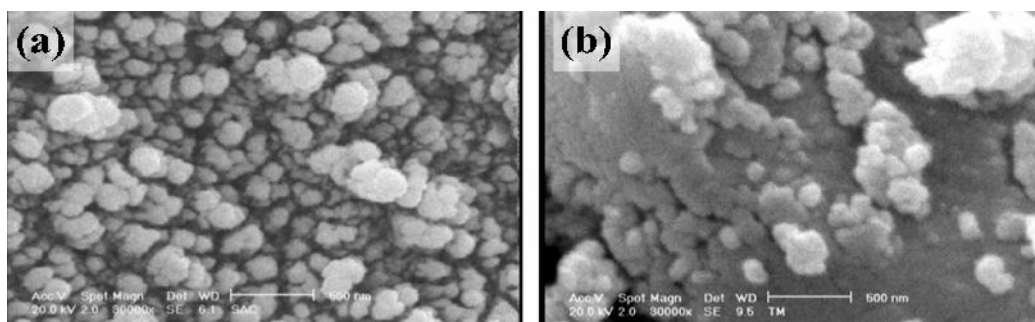


Fig. 4: SEM images of S-doped (a) and bare (b) TiO₂ nanoparticles

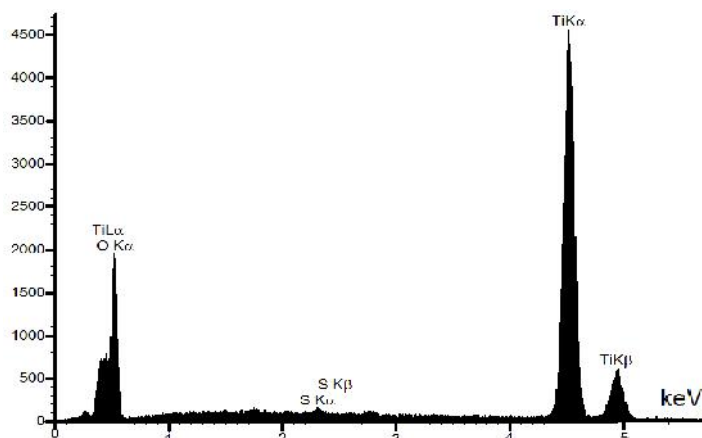


Fig. 5: EDX analysis of the S-doped TiO₂ nanoparticles.

transitions, respectively [20, 21]. The plots of $(ah\nu)^{1/2}$ for allowed indirect transitions of prepared S-doped TiO₂ (b) sample dispersed in ethanol versus photon energy are shown in Fig. 6. According to Fig. 6, the extrapolated optical absorption gap S-doped TiO₂ is found to be 2.8 eV at room temperature. The visible light absorbance of S-doped TiO₂ is of great significance for its practical application point of view. The estimated indirect band gap of the S-doped TiO₂ reveals 0.5 eV red shift from value reported in literature for bare TiO₂ [22, 23]. This phenomenon could be related to the mixing of the 3p states of sulfur with TiO₂ valence band (VB) causing an increase of (VB) width [17]. In the bare TiO₂ crystal, the valence band (VB) and conduction band (CB) consisted of the Ti3d and O2p orbitals. The Ti3d orbital was split in two parts (t_{2g} and e_g) states [20]. According to Umebayashi et al. obtained results, when TiO₂ was doped with sulfur, the 3p states of sulfur were somewhat delocalized. They also reported that the mixing of the 3p states with (VB) increased the width of the (VB) itself. So, sulfur

doping makes TiO₂ band gap to be narrowing [21, 23].

Fig. 7 shows the pore size distribution curve of S-doped TiO₂ nanoparticles calculated from a desorption branch of the nitrogen isotherm obtained by BJH (Barrett-Joyner-Halenda) method and its corresponding nitrogen adsorption-desorption isotherms (inset). According to inset of Fig. 7, isotherm is of type IV which proves the presence of mesopores within the synthesized sample [24]. The specific surface area of prepared material calculated to be 181.3 m²/g using the BET method and pore size distribution curve of the material obtained via BJH method revealed that the average diameter of the pores is 12.3 nm.

Photocatalytic activity performance

In photocatalytic experiments, 100 ml aqueous solution of Congo red (5 ppm) containing 0.05 g of photocatalyst was taken in the glass vessel under visible or ultraviolet light irradiation. The good visible light response of S-doped TiO₂ and its strong adsorption capability due to mesoporosity result a

catalyst with improved photocatalytic activity. Photocatalytic degradation of Congored causes its absorption bands to decrease with time, indicating the destruction of its chemical structure. Decrease of Congored concentration in photocatalytic systems was monitored by measuring the absorbance of the samples via UV-Vis spectrophotometer in different intervals. Fig. 8a and b shows changes of the UV-Vis absorption spectrum of Congored after adsorption of dye on S-doped TiO₂ at dark and during photocatalysis under ultraviolet and visible lights. It is observed that the intensity of the visible light chromophore band of Congo red, $\lambda = 497$ decreased as time passed and disappeared after 5 min of irradiation under either ultraviolet or visible light sources. Moreover, according to Fig. 8, visible light chromophore band of Congored undergoes a remarkable red shift during the course of photocatalytic degradation. This phenomenon is due to aggregation of Congored molecules in acidic conditions which is in accordance with our former reports [25]. Experiments had shown that Congored molecules exhibit an aggregate feature in acidic aqueous solutions with a red shift compared to monomer in UV-Vis absorption spectra due to dimmer molecules [25]. So, it is obvious that S-doping could enhance the surface acidity of TiO₂. These acidic sites could act as an electron acceptor, which would enhance the separation of the photo-generated charge carriers and improve the photocatalytic performance. This result is in accordance with Fengyu *et al.* findings [26].

Fig. 9 shows photocatalytic efficiency of S-doped

and bare TiO₂ for removal of dye solution as a function of time at $\lambda = 497$ nm under ultraviolet and visible lights. The efficiency or degree of photodecolorization (X) is given by: $X = (C_0 - C)/C_0$, where C_0 is the initial concentration of dye, and C is the concentration of dye at time T. The photocatalytic experiments using S-doped TiO₂ nanoparticle exhibited that not only sulfur modification makes the prepared photocatalyst to be active under visible light, but also more sensitized to ultraviolet light.

CONCLUSION

This research demonstrates the possibility of preparation of sol-gel mesoporous S-doped TiO₂ using titanium tetraisopropoxide, thiocarbamide and pluronic P123 surfactant as raw materials. S-doped TiO₂ prepared by this method has a highly crystalline single anatase phase and exhibits a high degree of mesoporosity that corresponds to a large surface area resulting in good photocatalytic properties. S-doping could lower the band gap of TiO₂ by the presence of an impurity state of S 3p on the upper edge of TiO₂ valence band. So that, the optical band gap of prepared S-doped TiO₂ estimated to be 2.8 eV that shows a large red shift compared to bare type. The prepared S-doped TiO₂ has good photocatalytic properties towards Congo red dye either under ultraviolet or visible light sources due to its anatase phase, narrowing of the band gap, acidic surface sites and large surface area.

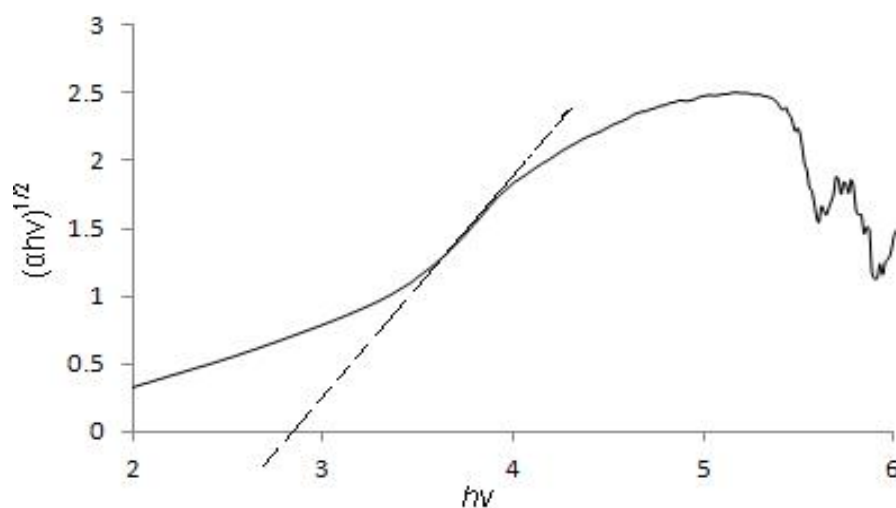


Fig. 6: $(\alpha hv)^{1/2}$ as a function of photon energy for prepared the S-doped TiO₂ sample dispersed in ethanol.

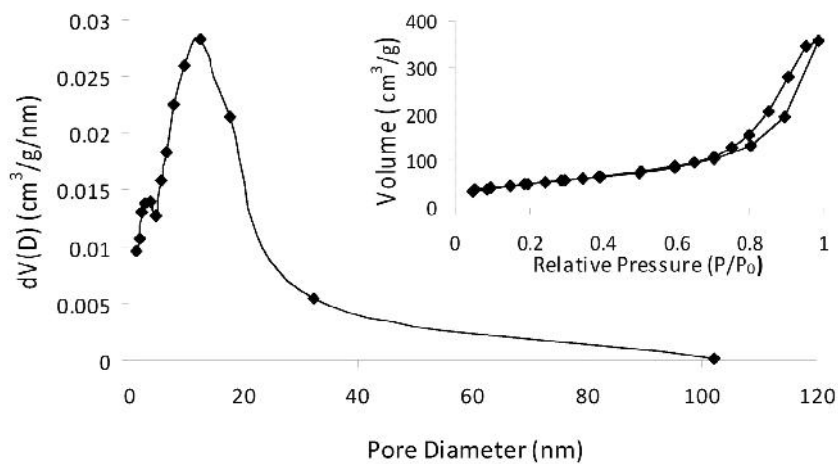


Fig.7: Pore size distribution curve of the S-doped TiO₂ nanoparticles - Inset: N₂ adsorption– desorption isotherm.

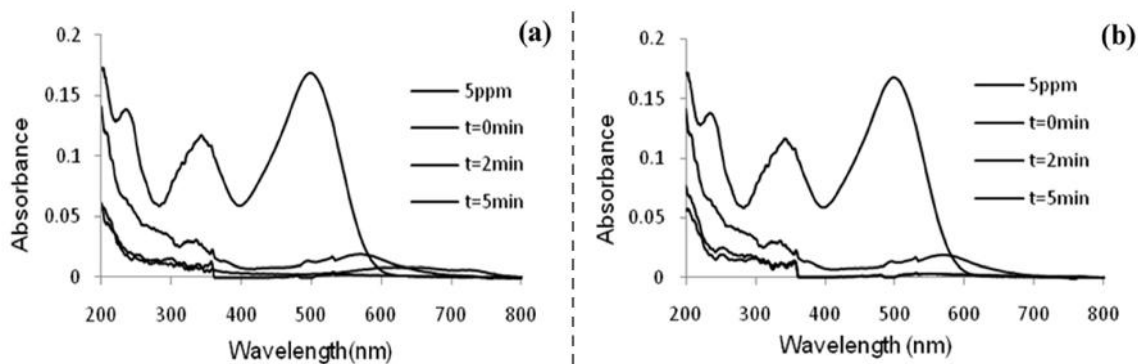


Fig. 8: Changes of UV-Vis spectrum of Congored in aqueous S-doped TiO₂ nanoparticles dispersion irradiated with a 30 W UV-C lamp light (a) and with two 18 W Osram lamps (b) as a function of time.

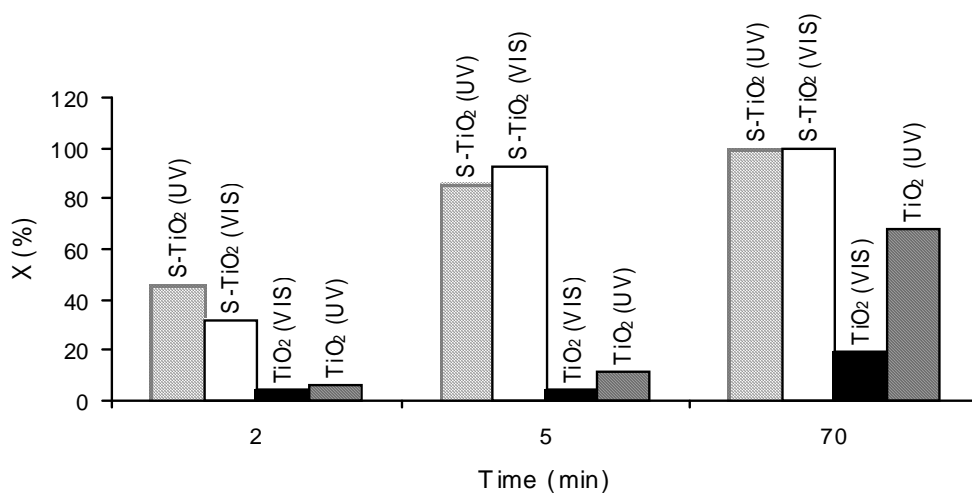


Fig. 9: Variation of photocatalytic activity of S-doped TiO₂ nanoparticles under ultraviolet and visible lights in comparison with bare TiO₂.

ACKNOWLEDGEMENT

Support by Nuclear Science and Technology Research Institute of Atomic Energy Organization of Iran and TarbiatModares University is greatly appreciated.

REFERENCES

- [1] Pei F., Liu Y., Xu S., Lu J., Wang C., Cao S., (2013), Nanocomposite of graphene oxide with nitrogen-doped TiO₂ exhibiting enhanced photocatalytic efficiency for hydrogen evolution. *Inter. J. Hydr. Energy*. 38: 2670-2677.
- [2] Tian H., Ma J., Li K., Li J., (2009), Hydrothermal synthesis of S-doped TiO₂ nanoparticles and their photocatalytic ability for degradation of methyl orange. *Ceramic Int.* 35: 1289-1292.
- [3] Hu S., Li F., Fan Z., (2011), The influence of preparation method, nitrogen source, and post-treatment on the photocatalytic activity and stability of N-doped TiO₂ nanopowder. *J. Hazard. Mater.* 196: 248-254.
- [4] Asiri A. M., Al-Amoudi M. S., Bazaid S. A., Adam A. A., Alamry K. A., Anandan S., (2014), Enhanced visible light photodegradation of water pollutants over N-, S-doped titanium dioxide and n-titanium dioxide in the presence of inorganic anions. *J. Saudi. Chem. Soc.* 18: 155-163.
- [5] Zhao B., Mele G., Pio I., Li J., Palmisano L., Vasapollo G., (2010), Degradation of 4-Nitrophenol (4-NP) Using Fe-TiO₂ as a Heterogeneous Photo-Fenton Catalyst. *J. Hazard Mater.* 176: 569-574.
- [6] Hamadani M., Reisi-Vanani A., Majedi A., (2010), characterization and effect of calcination temperature on phase transformation and photocatalytic activity of Cu,S-codoped TiO₂ nanoparticles. *Appl. Surf. Sci.* 256: 1837-1844.
- [7] Zhang Z., Wang X., Long J., Gu Q., Ding Z., Fu X., (2010), Nitrogen-doped titanium dioxide visible light photocatalyst: Spectroscopic identification of photoactive centers. *J. Catal.* 276: 201-214.
- [8] Janitabar-Darzi S., Mahjoub A. R., Nilchi A., (2009), Investigation of structural, optical and photocatalytic properties of mesoporous TiO₂ thin film synthesized by sol-gel templating technique. *Physica E*. 42: 176-181.
- [9] Wang Y., Li J., Peng P., Lu T., Wang L., (2008), Preparation of S-TiO₂ photocatalyst and photodegradation of L-acid under visible light. *J. Appl. Surf. Sci.* 254: 5276-5280.
- [10] Janitabar Darzi S., (2014), Mesoporous interstitial and substitutional nitrogen-containing titanium dioxide photocatalysts prepared by acid-assisted sol-gel procedure. *J. Iran. Chem. Soc.* 11: 1363-1371.
- [11] Ohno T., Tokieda K., Higashida S., Matsumura M., (2003), Synergism between rutile and anatase TiO₂ particles in photocatalytic oxidation of naphthalene. *Appl. Catal. A*. 244: 383-391.
- [12] Bu X., Wang Y., Li J., Zhang C., (2015), Improving the visible light photocatalytic activity of TiO₂ by combining sulfur doping and rectorite carrier. *J. Alloy. Compd.* 628: 20-26.
- [13] Zhang R., Gao L., (2002), Synthesis of nanosized TiO₂ by hydrolysis of alkoxide titanium in micelles. *Key. Eng. Mater.* 573: 224-226.
- [14] Klingenberg B., Vannice M. A., (1996), Influence of Pretreatment on Lanthanum Nitrate, Carbonate, and Oxide Powders. *Chem. Mater.* 8: 2755-2768.
- [15] Schrijnemakers K., Impens N. R. E. N., Vansant E. F., (1999), Deposition of a titania coating on silica by means of the chemical surface coating. *Langmuir*. 15: 5807-5813.
- [16] Wu W. C., Chuang C. C., Lin J. L., (2000), Bonding geometry and reactivity of methoxy and ethoxy groups adsorbed on powdered TiO₂. *J. Phys. Chem. B*. 104: 8719-8724.
- [17] Liu S., Chen X., (2008), Visible light response TiO₂ photocatalyst realized by cationic S-doping and its application for phenol degradation. *J. Hazard. Mater.* 152: 48-55.
- [18] Madarasz J., Braileanu A., Pokol G., (2008), Comprehensive evolved gas analysis of amorphous precursors for S-doped titania by in situ TG-FTIR and TG-DTA-MS. *J. Anal. Appl. Pyrolysis*. 82: 292-297.
- [19] Tonejc A. M., Turkovic A., Gotic M., Music S., Vukovic M., Trojko R., Tonejc A., (1997), HREM, TEM and XRD Observation of Nanocrystalline Phase in TiO₂ Obtained by the Sol-Jel Method. *Mater. Lett.* 31: 127-131.
- [20] Peercy P. S., (2000), The drive to miniaturization. *Nature*. 406: 1023-1026.
- [21] Wang D. J., Masuda Y., Seo W. S., Koumoto K., (2002), Metal-oxide-semiconductor (MOS) devices composed of biomimetically synthesized TiO₂ dielectric thin films. *Key. Eng. Mater.* 214: 163-168.
- [22] Janitabar Darzi S., Mahjoub A. R., Sarfi S., (2012), Visible- Light- Active Nitrogen Doped TiO₂ nanoparticles Prepared by Sol- Gel Acid Catalyzed reaction. *Iranian. J. Mater. Sci. Eng.* 9: 17-23.
- [23] Janitabar Darzi S., Mahjoub A. R., Hosseini A., (2010), Structural, Optical and Photocatalytic Properties of Sol-Gel Synthesized Mesoporous TiO₂ Film. *J. Nanosci. Nanotech.* 10: 1-5.
- [24] Umehayashi T., Yamaki T., Tanaka S., Asahi K., (2003), Visible light-induced degradation of methylene blue on S-doped TiO₂. *Chem. Lett.* 32: 330-331.
- [25] Movahedi M., Mahjoub A. R., Janitabar-Darzi S., (2009), Photodegradation of Congo Red in Aqueous Solution on ZnO as an Alternative Catalyst to TiO₂. *J. Iran. Chem. Soc.* 6: 570-577.
- [26] Fengyu W., Liangsoo N., Peng C., (2008), Preparation and characterization of N-S-codoped TiO₂ photocatalyst and its photocatalytic activity. *J. Hazard. Mater.* 156: 135-140.

How to cite this article: (Vancouver style)

Janitabar Darzi S., Mahjoub A. R., Bayat A., (2016), Synthesis and characterization of visible light active S-doped TiO₂ nanophotocatalyst. *Int. J. Nano Dimens.* 7(1): 33-40.

DOI: 10.7508/ijnd.2016.01.004

URL: http://ijnd.ir/article_15301_2444.html